Available online at www.sciencedirect.com
SCIENCE DIRECT
Journal of Magnetic Resonance 181 (2006) 331–335
JMR Journal of Magnetic Resonance
www.elsevier.com/locate/jmr

Communication

Indirect detection of nuclear magnetic resonance via geometrically induced long-range dipolar fields

C.A. Meriles *, Wei Dong

Department of Physics, CUNY—City College of New York, 138th Street and Convent Avenue, New York, NY 10031, USA

Received 25 February 2006; revised 14 April 2006
Available online 11 May 2006

Abstract

We report the indirect detection of the magnetization of one spin species via the NMR signal of a second species. Our method relies on the control of long-range dipolar fields between two separate objects, in this case, a water droplet (sensor) immersed in a tube containing mineral oil (sample). Unlike prior experiments, no gradient pulses are used; rather, the setup geometry is exploited to select the part of the sample to be probed and modulate the spin alignment in the sensor. Our results are discussed in the context of Dipolar Field Microscopy, a proposed strategy in which the detector is a hyperpolarized tip.

Keywords: Long-range dipolar fields; Dipolar Field Microscopy

Collective effects of the nuclear magnetization on the NMR spin dynamics were first reported by Deville, Bernier, and Delrieux [1]. In an experiment conducted almost thirty years ago, they observed and explained the unexpected string of echoes, following a standard two-pulse sequence in hyperpolarized ^{3}He. With the advent of improved higher-field NMR systems, non-linear nuclear spin dynamics became the subject of renewed attention as substantial effects were observed in protonated solutions at room temperature [2–8]. In the early 90's, Bowtell proposed a method for the indirect detection of one spin species via the demagnetizing field produced by spins in solution of a different species. Unlike other schemes, spins do not need to be part of the same molecule; in fact, the only requirement is that the two nuclear species be sufficiently close [4]. Extending these ideas, Warren et al. [7,9] and Bowtell et al. [10] showed that interactions can be established between nuclei of high gyromagnet ratios located in separate containers. In all these experiments, gradient pulses were used throughout the sequence to break the symmetry of the sample polarization by inducing a helical distribution of magnetization along the gradient pulse direction. A non-zero dipolar field is thus created and used to couple the analyte and the sensor nuclei. Broadly speaking, contributions to the dipolar field at every point originate mostly from nuclei contained in a sphere having a radius equal to the helix pitch [5]. Therefore, if sample and sensor nuclei reside in separate containers, the amount of coupling (i.e., the dipolar field of one nuclear species acting on the other) can be controlled by the duration of the gradient pulse.

Recently, one of us proposed that long-range dipolar couplings could serve as a tool for NMR microscopy [11]. In this scheme, the dipolar field of a small hyperpolarized tip placed in close contact with an extended sample is used to reorient the sample magnetization in the neighborhood of the tip. The result is a strong dipolar field at the tip site—this time, due to the sample—which is used in a second stage to modulate the tip magnetization. This approach could prove advantageous because highly sensitive methods can be used to probe the microtip and thereby, indirectly probe the sample with a resolution comparable to the size of the tip. As an initial demonstration of this methodology, we designed an experiment in which a ~3 mm diameter distilled water droplet—playing the role of the sensor—was used to detect the NMR signal of the

* Corresponding author. Fax: +1 212 650 7948.
E-mail address: cmeriles@sci.ccny.cuny.edu (C.A. Meriles).

1090-7807/$ - see front matter © 2006 Elsevier Inc. All rights reserved.
doi:10.1016/j.jmr.2006.04.009

sample surrounding the droplet, in the present case, silicone oil (Sigma–Aldrich) contained in a 5 mm diameter glass tube. Despite the change in geometry (the detection center is now embedded in the sample), the basic assumption of the scheme described above still holds: the sample (oil) and the detection center (water) are distinct and separate objects only connected through long-range intermolecular dipolar couplings. The scheme is reminiscent of previous work carried out by Pines and collaborators [12], who showed that hyperpolarized Xenon can be used as a sensor to pick up the signal of an analyte located in a separate container. Also, long-range dipolar fields in oil-water emulsions have been studied in the past by Cory and coworkers [13,14]. Nonetheless, the context and motivation are markedly different in this experiment. Furthermore, our strategy uses only the geometry of the setup to generate and detect the dipolar field interaction, i.e. no symmetry-breaking field gradient pulses are utilized.

Fig. 1 shows the pulse sequence used: selective excitation of the oil protons initiates the evolution of the sample magnetization in the presence of the dipolar field due to the water droplet. In the frame rotating at the oil Larmor frequency, only nuclei neighboring the water droplet are affected by its dipolar field. The contact time $t_{c1} = 3\pi/(4\gamma\mu_0 M^0_{\mathrm{det}})$ is chosen so that sample nuclei located close to the poles of the water droplet total a $\pi/2$ rotation during the first interval. In the above expression, M^0_{det} is the equilibrium magnetization of the detector, γ is the proton gyromagnetic ratio and μ_0 is the vacuum magnetic permeability. In a magnetic field of 9.4 T (400 MHz ^{1}H resonance frequency) at room temperature we have $t_{c1} \sim 300$ ms. It is not difficult to demonstrate that the sample magnetization parallel to the main magnetic field (z-axis) at the end of the encoding period is given by $M^{(z)}_{\mathrm{spl}}(t_{c1}) = M^0_{\mathrm{spl}} \sin(\frac{\pi}{4}(\frac{r_0}{r})^3 (3\cos^2\theta - 1))$. Here, M^0_{spl} is the equilibrium sample magnetization; r_0 is the water droplet radius; r is the distance to the droplet center and θ is the angle with the main magnetic field direction. The strongly inhomogeneous distribution of sample magnetization induces a rather homogeneous dipolar field on the water droplet. A full numerical calculation shows that this field reaches a magnitude equal to $B^{\max}_{\mathrm{spl}} = 2.3\mu_0 M^{(0)}_{\mathrm{spl}}/(4\pi)$ with a variation of approximately $\pm 10\%$ over the droplet volume. At 9.4 T for a room-temperature silicone-oil sample, $B^{\max}_{\mathrm{spl}}$ amounts to roughly 5.9 nT (0.25 Hz ^{1}H frequency).

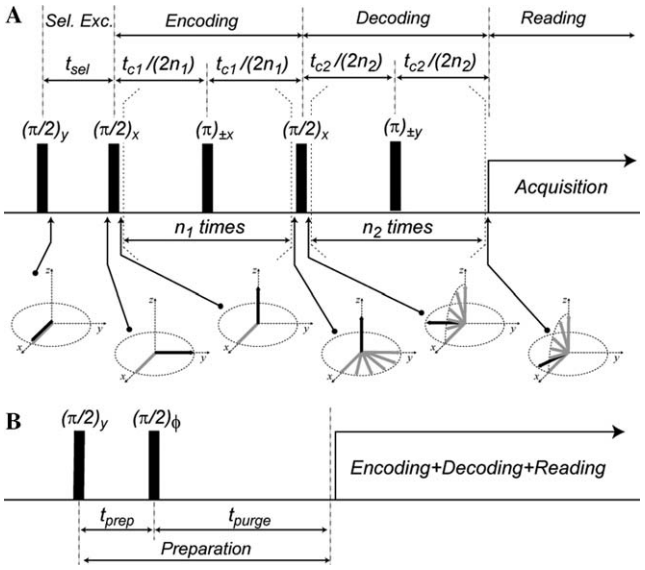

Fig. 1. (A) Pulse protocol for indirect detection of the sample magnetization. During the 'encoding' period, sample spins (indicated by gray arrows) evolve in the presence of the dipolar field due to the sensor. The gained phase depends on the position of the sample spin relative to the water droplet. A $\pi/2$ 'transition pulse' at the end of this period simultaneously excites water spins (black arrows) and generates a non-homogeneous distribution of sample magnetization along the z-axis. This induces a dipolar field on the sensor, which translates into a slow precession of the water nuclei. Trains of π-pulses with alternating phase during the 'encoding' and 'decoding' intervals are used to eliminate the effect of field inhomogeneities (or frequency offset). An even number of pulses has been assumed to simplify the drawing but this condition is unnecessary. Acquisition starts at the last echo point. Selective excitation of sample nuclear spins was carried out using a pair of phase-shifted $\pi/2$-pulses; t_{sel} was chosen as 1/4 the inverse of the frequency difference between the oil and water resonances (0.13 ms). (B) A 'preparation' interval preceding the pulse sequence in (A) is used to control the initial sample magnetization along the z-axis. The phase ϕ is chosen so that, irrespective of t_{prep}, sensor spins point along the $+z$ direction after the second $\pi/2$-pulse; a purge period t_{purge} of 100 ms was used in all cases to eliminate remaining in-plane sample magnetization.

The presence of an additional external magnetic field acting on the water nuclei translates into a slow evolution of the water magnetization during t_{c2}. It is worth pointing out that the synchronous inversion of the sample and sensor magnetization during this (and the former) time interval eliminates dephasing induced by field inhomogeneities but preserves the action of the dipolar field. The expected result is a slow precession of the sensor spins at the frequency of the sample dipolar field. Fig. 2 shows the spectrum of the signal recorded after t_{c2}. The oil peak—here kept as a reference for demonstration purposes—is due to in-plane magnetization originating from nuclei only weakly affected by the water dipolar field during the encoding period. After short time intervals, the water signal shows a 90° phase shift relative to the oil peak, a simple consequence of the phase difference introduced at time t_{c1} during excitation of the water nuclei. As the contact time t_{c2} increases, however, this phase shift progressively diminishes until the water peak becomes in phase with the oil peak at about 1.4 s. No significant changes are observed at later times; after 2 s of evolution, a low signal to noise ratio makes detection impractical.

These results are in good agreement with our model: taking 1.4 s as the time needed to induce a $\pi/2$-rotation of the water nuclei, the *effective* dipolar field due to the sample during the decoding period amounts to 0.17 Hz. This number is considerably smaller than the crude estimate indicated above (0.25 Hz) but the agreement improves significantly if the various mechanisms of relaxation are taken into account. For example, when longitudinal and transverse relaxation times (identical for an isotropic liquid) are considered [15], a full numerical simu-

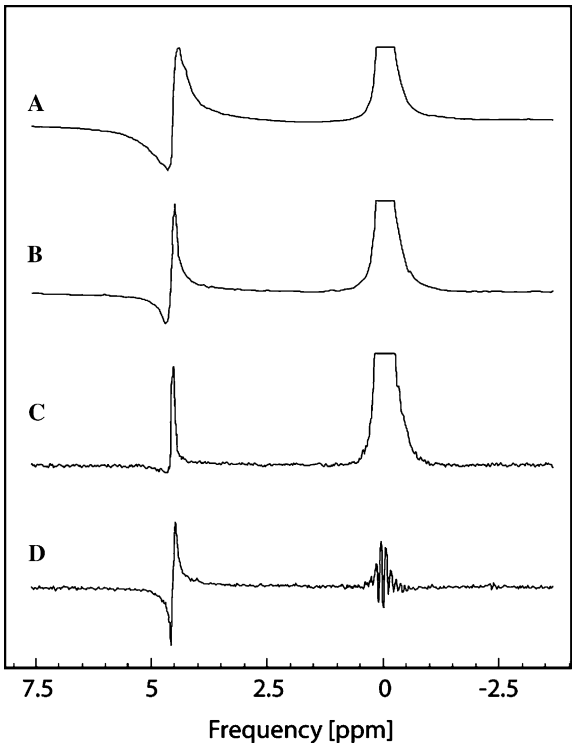

Fig. 2. Fourier transform of the signal detected after a variable decoding time; t_{c2} was set to 200 ms in (A), 700 ms in (B) and 1400 ms in (C). The evolution of the sensor spins in the presence of the sample dipolar field appears as a slow phase shift of the water peak. The phase of the oil resonance peak—shown truncated and used as a reference—remains undistorted. In all three cases a preparation time of only 5 μs was used leaving both the oil and the water initial magnetization undistorted. A purge time of 100 ms was used; the number of scans was 16. The number of echoes n_1 and n_2 were 3 and 7, respectively. (D) Same as in (C) but with t_{prep} chosen to saturate the sample spins (0.13 ms). In the absence of an external dipolar field, the water resonance peak exhibits no phase shift.

lation of the spin dynamics in this system [16] yields an effective dipolar field of 0.19 Hz. Pulse imperfections during the sequence (particularly during the trains of π-rotations in the encoding and decoding periods) further decrease this value. Note that although a single inversion is necessary to eliminate the effect of field inhomogeneities (much stronger than the dipolar field to be measured), several π-pulses are preferred in practice. This is because damping of the measured signal due to self-diffusion can be lessened by decreasing the free evolution time between inversions, therefore improving the signal-to-noise ratio to a level compatible with our detection sensitivity. It is worth pointing out, nonetheless, that self-diffusion effects are not expected to considerably attenuate the (relevant) dipolar field neither during t_{c1} nor t_{c2}. Water self-diffusion is unimportant both during the encoding period (because the droplet dipolar field remains unaltered) and throughout the decoding time interval (because the oil dipolar field is fairly homogenous). On the other hand, oil exhibits a self-diffusion coefficient considerably smaller than that of water making diffusion effects rather negligible for the time scale and physical dimensions of the system under consideration.

The ability to indirectly detect the oil NMR signal by inspecting the water sensor is shown in Fig. 3. Here, the pulse sequence is preceded by a preparation interval in which the oil magnetization is manipulated to modify the state prior to the encoding period. A 100 ms purge time between the preparation and encoding pulses was used to eliminate remaining in-plane oil magnetization. The phase of the 'transition' pulse at t_{c1} was changed by 180° in even-numbered acquisitions to cancel the imaginary component of the water signal (see Fig. 1). The result is that the sensor signal will be non-zero only when an external dipolar field is present; further, the sign of the water peak will reflect the alignment (along the z-axis) of the sample nuclei inducing this field. In case 3a, the short preparation time used (5 μs) leaves the oil magnetization unchanged and consequently, the water peak appears in-phase. Almost no signal is detected in case 3b, because the preparation time (0.13 ms) was chosen to saturate the oil spins; i.e., no dipolar field was acting on the droplet during t_{c2}. Finally, the water peak changes sign in case 3c reproducing the inver-

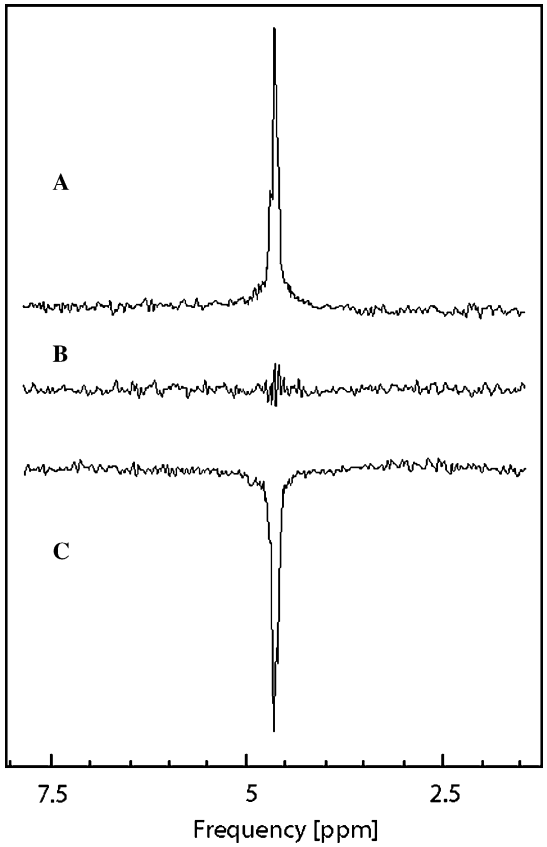

Fig. 3. When the phase of the 'transition pulse' (third π/2-pulse in Fig. 1A) changes 180° in every scan, the dispersive component of the water signal is averaged out (after an even number of acquisitions). Therefore, the amplitude of the resulting absorptive sensor peak becomes proportional to the sample magnetization as set in the preparation period. In (A), the sample magnetization is left unchanged using $t_{prep} = 0.005$ ms; it becomes zero in (B) setting $t_{prep} = 0.13$ ms and is inverted in (C) with $t_{prep} = 0.26$ ms. In all cases, t_{purge} was 100 ms and the total number of scans was 32. The number of echoes n_1 and n_2 were 3 and 7, respectively.

sion of the sample magnetization during the preparation interval ($t_{prep} = 0.26$ ms). Note that the signal amplitude is comparable to that of case 3a. This is consistent with the short overall increment of the sequence duration relative to the sample and sensor relaxation times (roughly 2 s).

Indirect detection of nuclear magnetic resonance as reported here could become a valuable strategy if the sensor is engineered to enable the use of detection methods more sensitive than standard Faraday induction [11]. For example, detection of the nuclear polarization at the nanoscale has been demonstrated using electrical methods [17] and is currently investigated by several groups [18]. Further, Optical Faraday Rotation [19] and luminescence-based schemes [20,21] have been used to probe the nuclei contained in a semiconductor heterostructure [22] or in a single quantum dot [23]. In the present context, the high sensitivity common to these detection strategies could be exploited to locally probe an arbitrary sample (having non-zero nuclear spins) through a sensor optimized to provide the best possible signal. Clearly, various geometries are conceivable although a tip/sample configuration is particularly appealing and has been the subject of our recent study [11]. Because the size of the probed sample is comparable to the size of the tip, a spatial resolution exceeding that attained by standard schemes could be possible. Dipolar Field Microscopy (DFM)—the name we have suggested for this strategy—could thus be used to reconstruct images as the tip scans the sample. Alternatively, it could be used to reconstruct a local high-resolution NMR spectrum if the preparation interval preceding the detection protocol (encoding and decoding periods) is sequentially incremented.

The results reported in this manuscript are insufficient to address the many technical questions associated with the practical implementation of DFM though they provide a starting point and a demonstration of the underlying physics: nuclear dipolar fields originating in the geometry of the setup can be used to couple two separate (but close) objects and indirectly determine the magnetization of one of them by its effect on the other. Certainly, both the sensor and the sample will be solids at the low temperatures required for DFM and thereby it can be argued that the shorter transverse relaxation times will render our approach impractical. This argument, however, is inaccurate: orders-of-magnitude increased magnetizations are possible by cooling the sample and dynamically polarizing the sensor, which correspondingly leads to contact times much shorter than those reported here ($t_{c1} \sim 1$ ms and $t_{c2} \sim 100$ ms for a 10% polarized GaAs tip close to a sample at 4 K in a 10 T magnet). On the other hand, transverse relaxation times reaching up to 2 s have been attained by combining homonuclear spin decoupling with cyclic inversions [24].

Although the practical implementation of our scheme in a solid is technically more demanding, the use of liquid samples as reported here makes the conceptual analysis of this experiment comparatively more complex. This is because it is not evident whether non-linear effects due to internal demagnetizing fields in the sample and detector can be neglected during the spin evolution. It is not very difficult, however, to qualitatively demonstrate that this is indeed the case: In our setup, the field inhomogeneity (approximately 60 Hz FWHH) is tens of times larger than the magnitude of the inner demagnetizing fields (less than 1 Hz). The result is that the in-plane components of this field will be effectively averaged away; only the z-component of the inner demagnetizing field in the sample (sensor) must be considered during the encoding (decoding) time interval. A simple calculation demonstrates that this component is zero when the sample (sensor) magnetization lies along the xy-plane, which is practically the case during t_{c1} (t_{c2}). A full numerical simulation that takes into account the spatial configuration in our system further supports this conclusion. These results [16]—not included here for brevity—indicate that the inner dipolar field will be weak even in the case in which the main magnetic field is perfectly homogeneous (due to the singular geometry of our experimental setup). A full account of these and other details is in preparation and will be published elsewhere.

From a more general perspective, an interesting feature of the proposed scheme is that the role played by the sample magnetization is merely to define the contact time necessary to modulate the sensor magnetization. Thus, as long as relaxation can be ignored, the detection sensitivity does not depend on the sample magnetization but only on our ability to pick-up the sensor signal (which, as mentioned, can be favorably engineered). This contrasts with standard Faraday detection: if S and F, respectively, represent the signal-to-noise ratio obtained with standard inductive detection and the proposed method, S drops by half when the sample magnetization is reduced by the same amount. In the proposed scheme, however, one can double the contact time t_{c2} in which case F will remain unchanged. In other words, within the limits imposed by relaxation, it is possible to trade contact time in a single scan to gain a better signal-to-noise ratio. At the low temperatures required for DFM, this feature could prove beneficial in various applications, for example, to characterize dilute samples.

Acknowledgments

The authors gratefully acknowledge Boris Itin and Phillip Stallworth for valuable assistance during these experiments. CAM and WD are members of the New York Structural Biology Center, which is supported by the New York State Office of Science, Technology and Academic Research, and National Institutes of Health Grant P41 FM66354.

References

[1] G. Deville, M. Bernier, J.M. Delrieux, NMR multiple echoes observed in solid ^{3}He, Phys. Rev. B 19 (1979) 5666–5688.
[2] H.T. Edzes, The nuclear magnetization as the origin of transient changes in the magnetic field in pulsed NMR experiments, J. Magn. Reson. 86 (1990) 293.

[3] R. Bowtell, R.M. Bowley, P. Glover, Multiple spin echoes in liquids in a high magnetic field, J. Magn. Reson. 88 (1990) 643.
[4] R. Bowtell, Indirect detection via the dipolar demagnetizing field, J. Magn. Reson. 100 (1992) 1.
[5] W.S. Warren, W. Richter, A.H. Andreotti, B.T. Farmer, Generation of impossible cross peaks between bulk water and biomolecules in solution NMR, Science 262 (1993) 2005.
[6] A. Vlassenbroek, J. Jeener, P. Broekaert, Macroscopic and microscopic fields in high-resolution liquid NMR, J. Magn. Reson. Ser. A 118 (1996) 234.
[7] W. Richter, S. Lee, W.S. Warren, Q. He, Imaging with intermolecular zero-quantum coherences in solution nuclear magnetic resonance, Science 267 (1995) 654.
[8] For a review, see M.H. Levitt, Demagnetization field effects in two-dimensional solution NMR, Concepts Magn. Reson. 8 (1996) 77.
[9] X.P. Tang, C.L. Chin, L.S. Bouchard, F.W. Wehrli, W.S. Warren, Observing Bragg-like diffraction via multiple couple nuclear spins, Phys. Lett. A 326 (2004) 114.
[10] R. Bowtell, S. Gutteridge, C. Ramanathan, Imaging the long-range dipolar field in structural liquid state samples, J. Magn. Reson. 150 (2001) 147.
[11] C.A. Meriles, Optically-detected Nuclear Magnetic Resonance at the sub-micron scale, J. Magn. Reson. 176 (2005) 207.
[12] J. Granwehr, J.T. Urban, A.H. Trabesinger, A. Pines, NMR detection using laser-polarized xenon as a dipolar sensor, J. Magn. Reson. 176 (2005) 125.
[13] S.M. Brown, P.N. Sen, D.G. Cory, Scaling Laws in NMR scattering via dipolar fields, J. Magn. Reson. 154 (2002) 154.
[14] S.M. Brown, P.N. Sen, D.G. Cory, Nuclear Magnetic Resonance scattering across interfaces via the dipolar demagnetizing field, J. Chem. Phys. 116 (2002) 295.
[15] Oil and water longitudinal relaxation times where determined through standard inversion-recovery pulse sequences; this experiment yielded 1.6 s and 2.4 s, respectively.
[16] A set of Bloch equations modified to include non-linear effects due to the nuclear dipolar field has been numerically solved applying a fourth order Runge-Kutta algorithm. Spins were distributed on a cartesian grid that reproduced the geometry discussed in this paper.
[17] M. Dovers, K.V. Klitzing, J. Schneider, G. Weinman, K. Ploog, Electrical detection of Nuclear Magnetic Resonance in GaAs–$Al_xGa_{1-x}As$ heterostructures, Phys. Rev. Lett. 61 (1988) 1650.
[18] J.A. Nesteroff, Y.V. Pershin, V. Privman, Polarization of nuclear spins from the conductance of a quantum wire, Phys. Rev. Lett. 93 (2004) 126601.
[19] S.A. Crooker, D.D. Awschalom, J.J. Baumberg, F. Flack, N. Samarth, Optical spin resonance and transverse spin relaxation in magnetic semiconductor quantum wells, Phys. Rev. B 56 (1997) 7574.
[20] J.A. Marohn, P.J. Carson, J.Y. Hwang, M.A. Miller, D.N. Shykind, D.P. Weitekamp, Optical Larmor beat detection of high-resolution nuclear magnetic resonance in a semiconductor heterostructure, Phys. Rev. Lett. 75 (1995) 1364.
[21] M. Eickhoff, D. Suter, Pulsed optically detected NMR of single GaAs/AlGaAs quantum wells, J. Magn. Reson. 166 (2004) 69.
[22] J.M. Kikkawa, D.D. Awschalom, All-optical magnetic resonance in semiconductors, Science 287 (2000) 473.
[23] D. Gammon, S.W. Brown, E.S. Snow, T.A. Kennedy, D.S. Katzer, D. Park, Nuclear spectroscopy in single quantum dots: nanoscopic Raman scattering and nuclear magnetic resonance, Science 277 (1997) 85.
[24] This time corresponds to an isotopically enriched (97%) sample of ^{29}Si. Coherences lasting up to 30 s were observed in natural silicon. See T.D. Ladd, D. Maryenko, Y. Yamamoto, Coherence time of decoupled nuclear spins in silicon, Phys. Rev. B 71 (2005) 014401.